Comparison of soil moisture in GLDAS model simulations and satellite observations over the Murray Darling Basin

Liu, Y. Y. [1, 3], M. F. McCabe [1], J. P. Evans [2], A. I. J. M. van Dijk [3], R. A. M. de Jeu [4] and H. Su [5]

[1] School of Civil and Environmental Engineering, University of New South Wales, Sydney
[2] Climate Change Research Centre, University of New South Wales, Sydney
[3] CSIRO Land and Water, Black Mountain Laboratory, Canberra
[4] Department of Hydrology and Geo-Environmental Sciences, Faculty of Earth and Life Sciences, Vrije Universiteit Amsterdam, Amsterdam, Netherlands
[5] Center for Research on Environment and Water (CREW), Calverton, Maryland, USA
Email: yi.liu@student.unsw.edu.au

Abstract: Soil moisture is a key hydrometeorological variable that can be derived from both modeling simulations and satellite observations. This study compares Global Land Data Assimilation System (GLDAS) output over the Murray Darling Basin against retrievals from a newly developed remote sensing product using the AMSR-E sensor onboard NASA's Aqua satellite. GLDAS is comprised of a number of land surface models, two of which include the Community Land Model (CLM) and NOAH land surface scheme, which provide a temporally and spatially consistent characterization of the hydrological cycle. GLDAS derived estimates are 3-hourly products with 0.25-degree spatial resolution, while satellite based observations offer twice-daily instantaneous retrievals at similar spatial scales. The models represent different soil moisture averaging depths (roughly 2, 5, and 10 cm in CLM and 10 cm in NOAH) and retrievals from AMSR-E C-band approximate the soil moisture in the top 1.5 cm layer. The spatial distribution and coherence of soil moisture are investigated seasonally and under both wetting and drying conditions. From the spatial aspect, AMSR-E observations and GLDAS simulations show similar seasonal patterns, while simulated soil moisture is slightly higher during summer and autumn over the north-eastern Murray Darling Basin (MDB). This may be explained by the positive biases of GLDAS forcing precipitation data. From the temporal perspective, the best match between AMSR-E soil moisture and model simulations is found over the regions with strong precipitation in warm months, e.g. north-eastern MDB. Over the regions with high precipitation during cool months, AMSR-E soil moisture is systematically higher than model simulations. For the regions with extremely low annual rainfall, the peak values in soil moisture between AMSR-E and model simulations match very well, while low values of soil moisture display the greatest differences.

Generally, the agreements between AMSR-E observations and GLDAS simulations vary under different wetting and drying conditions. Both of them can represent the 'true' soil moisture to some extent. How to best blend soil moisture products derived from these two different techniques, in addition to data assimilation approaches, will be explored in future research.

Keywords: *Soil moisture, CLM, NOAH, AMSR-E, Murray Darling Basin*

1. INTRODUCTION

Soil moisture is a key hydrometeorological variable in many hydrological processes. Accurate measurements of soil moisture can help to predict runoff, infiltration, evaporation and other important variables. (Cashion et al. 2005). Soil moisture over large scale can be derived from satellite observations and modelling simulations. Among remote sensing techniques, the microwave domain is favourable for soil moisture retrievals, as it can penetrate cloud and can provide information on water content of the top soil layer, rather than the land surface only. Within the microwave domain, lower frequencies can penetrate more deeply and are less attenuated by vegetation, thus the soil moisture retrieved from lower microwave frequencies is expected to be more accurate. The Advanced Microwave Scanning Radiometer – Earth Observation System (AMSR-E) sensor onboard NASA's Aqua satellite has the lowest passive microwave frequency among the currently operational satellites. There are several algorithms to retrieve soil moisture using the AMSR-E observed brightness temperature. Draper et al. (2009) illustrates that the soil moisture retrievals from the algorithm developed by the Vrije Universiteit Amsterdam (VUA), in comparison with NASA-JPL approach, has a better correspondence to the in-situ data over the south-eastern Australia. Therefore, the AMSR-E soil moisture product from the VUA-NASA algorithm is applied in this study.

The Global Land Data Assimilation System (GLDAS) was developed jointly by scientists from NASA and NOAA, aiming to accurately simulate water and energy cycle states and fluxes (Rodell et al., 2004). The uniqueness of GLDAS is that it is a global, high resolution, offline terrestrial modelling system incorporating ground and satellite observations. GLDAS includes four land surface models: the Community Land Model (CLM), NOAH, Mosaic, and the Variable Infiltration Capacity (VIC) model. Due to the data availability, only CLM and NOAH models are used in this analysis.

This study compares the soil moisture derived from AMSR-E sensor and that from top soil layers in CLM and NOAH land surface schemes over the Murray Darling Basin (MDB). Section 2 briefly describes the MDB, AMSR-E soil moisture, CLM and NOAH land surface schemes, and other variables involved in this analysis. In section 3, we present the spatial and temporal patterns of the comparison results. Section 4 discusses the reasons for the discrepancies between satellite observations and modelling simulations.

2. DATA AND METHODS

2.1 Murray Darling Basin (MDB)

The MDB (Figure 1) is located in south-eastern Australia. It is one of Australia's largest drainage divisions and covers one-seventh of the continent. The MDB is important for Australia's community and economy, as three million people inside and outside the MDB are directly dependent on its water and more than 80% of all irrigation in Australia takes place in the MDB. However, its long-term productivity and sustainability is under threat from over-allocated water resources, salinity and climate change (http://www.environment.gov.au/water/mdb). This makes the investigations of water resources over the MDB, including all hydrological components, more important.

Figure 1. Location of Murray Darling Basin (MDB).

2.2 AMSR-E soil moisture

AMSR-E was launched in May 2002 and has six microwave frequencies, only four of which are relevant to soil moisture retrievals: 6.9 (C-band), 10.6, 18.7 and 36.5 GHz. The swath width is roughly 1445 km and the overpass time is around 1:30 am for ascending and 1:30 pm for descending swaths, which results in almost 100 percent daily global coverage when combining ascending and descending swaths. We used the top 1.5-cm soil moisture retrieved using the VUA-NASA Land Parameter Retrieval Model (LPRM) and C-band brightness temperature (Owe et al., 2008). The C-band soil moisture was re-sampled into 0.25-degree (about 25 km) spatial resolution from the original 74×43 km^2 resolution. Daily average is taken by combining both ascending and descending swaths, and the original soil moisture retrievals are directly used without any modification. Monthly and seasonal averages are calculated from the daily average for the study period (December 2003 through November 2005).

2.3 CLM and NOAH land surface schemes

As models driven in GLDAS, the CLM and NOAH use the same static and forcing input data, and simulate soil moisture, soil temperature, skin temperature, snow melting, snow water equivalent, canopy water content, and the energy flux and water flux terms of the surface energy balance and surface water balance. CLM and NOAH have ten and four vertical levels, respectively. For better comparison with the near-surface soil moisture from AMSR-E, the vertical layers used here include 10-cm soil layer in NOAH and roughly 2, 5, and 10-cm soil layers in CLM. The CLM and NOAH models are run at a spatial resolution of 25 km. Daily averages are obtained by integrating 3-hourly simulation outputs, and monthly and seasonal averages are calculated from daily average.

Near surface soil moisture is expected to be highly related with precipitation. Here we include two precipitation data sets for comparison purposes: gridded rainfall data across Australia were interpolated from point observations by the Queensland Department of Natural Resources and Mines (QDNRM, http://www.nrw.qld.gov.au/silo/datadrill/), also known as SILO rainfall, and GLDAS precipitation data derived from Global Data Assimilation System (GDAS) reanalysis.

2.4 Statistic methods

K-means clustering algorithm was applied on the monthly SILO precipitation over the MDB to classify regions with different precipitation patterns. Spearman's (non-parametric) correlation analysis was used in this study to investigate the correlations between monthly soil moisture from AMSR-E observations and CLM/NOAH simulations. This was chosen because it does not require any assumptions about the nature of the relationship, as long as it is monotonic. The root mean squared error (RMSE) was also calculated to assess the differences between monthly AMSR-E observations and modelling simulations.

3. RESULTS

Figure 2 shows that the western parts are consistently dry and the east MDB is relatively wet, while north-eastern and south-eastern MDB have different rainy seasons. This section compares the seasonal soil moisture over the entire MDB and the temporal patterns for three selected pixels shown as black stars in Figure 2. The three pixels are selected to investigate the relationships between AMSR-E observations and modelling simulations under different precipitation conditions.

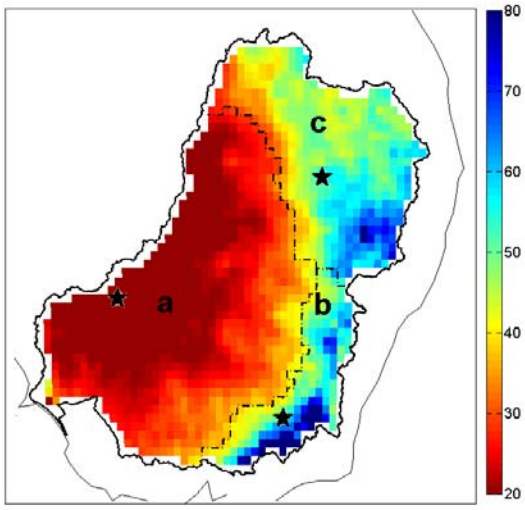

Figure 2. Monthly average rainfall (mm/month) for the study period (December 2003 through November 2005), calculated from SILO rainfall. Regions (a, b and c) delineated by the dash-dot lines represent different precipitation patterns, derived from k-means clustering analysis. The annual precipitation in region (a) is extremely low and dominated by several rainfall events. Region (b) and (c) have greater annual precipitation, while most rainfall events occur during winter and spring for region (b) and during summer and autumn for region (c).

3.1 Spatial patterns

Seasonal averages of top layer soil moisture (Figure 3) from AMSR-E observations and CLM/NOAH simulations show similar spatial patterns. The highest soil moisture is observed over south-eastern MDB in winter resulting from the relatively high rainfall and low evaporation. Over the north-east MDB, the soil moisture is highest during summer when most precipitation events occur. Spring and autumn are the transitional seasons in between. It is noted that during summer and autumn, simulated soil moisture over north-east MDB seems higher than AMSR-E observations. This is likely related to the positive bias of GLDAS forcing precipitation data (presented in section 4).

Although they show similar spatial patterns, the ranges of variations between shallow and deep soil layers are different. The top 2-cm soil moisture varies with precipitation and evaporation more quickly than deeper soil layers, thus they have greater variations as shown in Figure 3 (first two columns). Soil moisture in the deeper

soil layers has relatively longer memory (last three columns in Figure 3). For the 5, 10-cm in CLM and 10-cm in NOAH, the high soil moisture in winter (summer) can still be observed in spring (autumn). The comparison of seasonal averages of soil moisture for 2005 (not presented here) is similar to 2004.

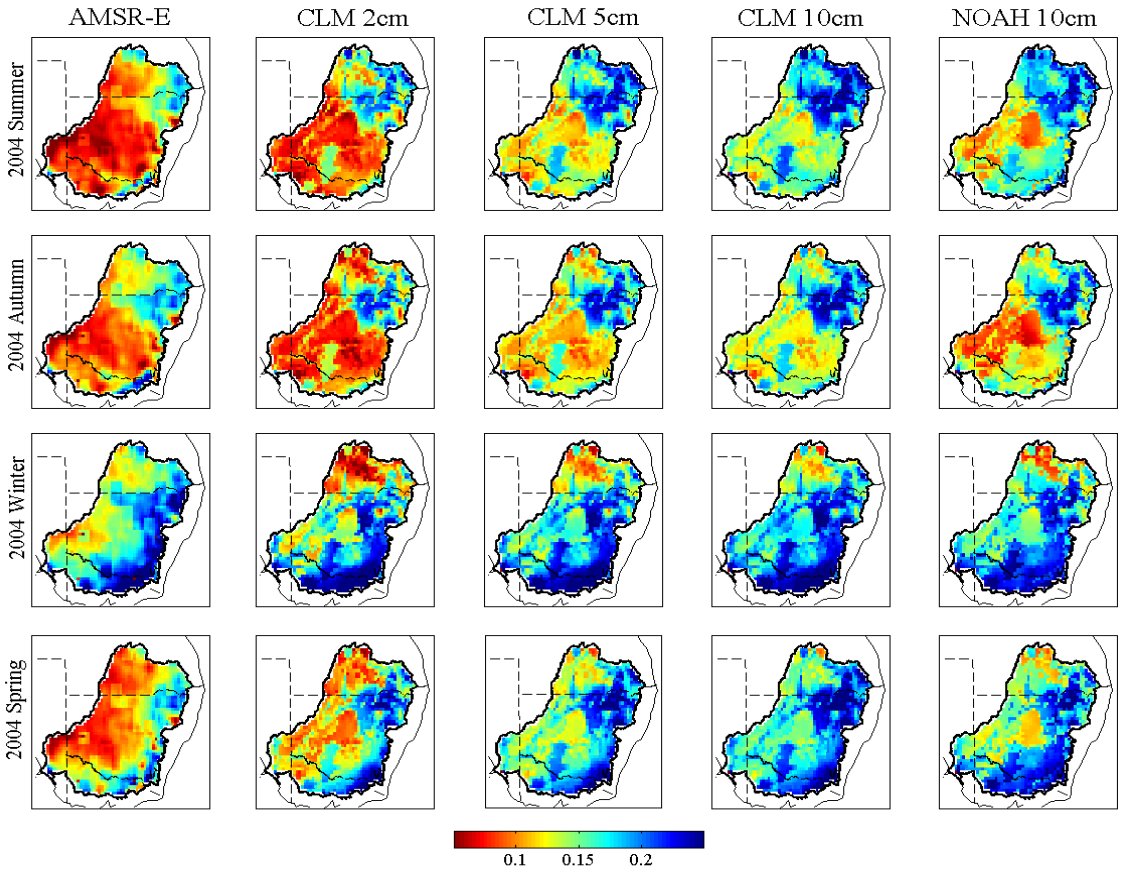

Figure 3. From left to right column, AMSR-E near surface soil moisture, CLM top layer moisture (2, 5, 10 cm) and NOAH 10-cm soil moisture. From top to bottom, Summer, Autumn, Winter and Spring for 2004.

3.2 Temporal patterns

The three selected pixels represent regions with different precipitation conditions. As stated, precipitation in region (a) is lower than (b) and (c), dominated by only several events in winter and spring. Region (b) has a larger number of precipitation events, most of which occur in winter and spring. Region (c) also has high annual precipitation with high rainfall events during summer and autumn.

All simulated soil moisture patterns have similar peak values corresponding to precipitation events, but different base values, dependent on the depth of soil layers. Deeper soil layers have higher base values, even though for the same soil layer (10 cm in our case), the base values and recession rates may vary in different models.

Figure 4a shows the peak values in soil moisture from AMSR-E observations, with corresponding simulations matching well. However, there are apparent discrepancies during the low value periods which can be observed. This is particularly so during summer and autumn when it is the dry season for region (a): the AMSR-E soil moisture is lower than the lowest base value in CLM, and it has an upward trend. In Figure 4b, the AMSR-E soil moisture and model simulations agree reasonably well in the relatively dry season. During the wet season, the discrepancies in the peak values are striking, with AMSR-E soil moisture is routinely higher than model simulations. Figure 4(c) indicates that the AMSR-E soil moisture and model simulations are consistently in agreement.

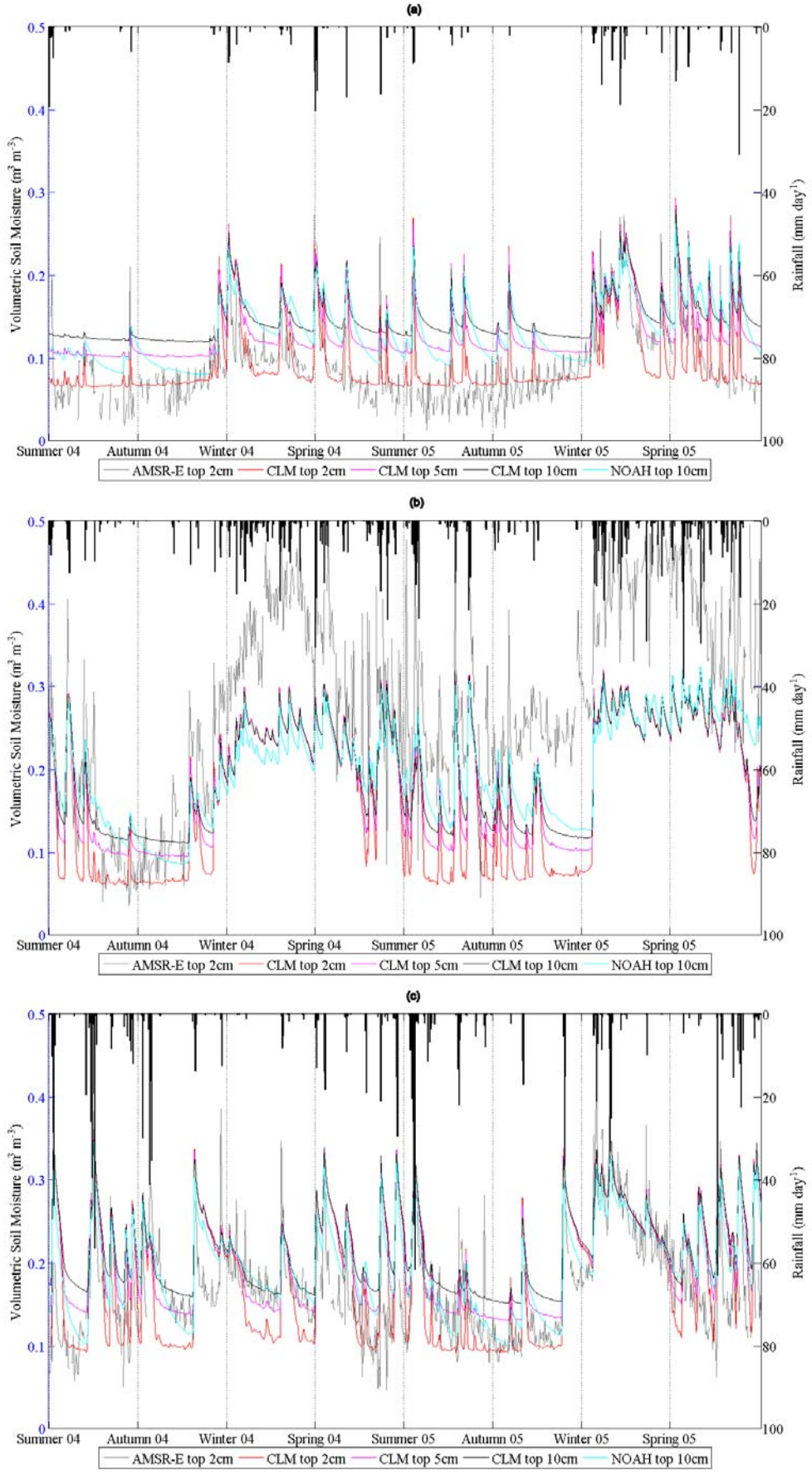

Figure 4. Daily soil moisture from AMSR-E observations and CLM/NOAH simulations for three selected pixels as shown in Figure 2. (a) from the west MDB, (b) from the south-east MDB and (c) from northern MDB.

To compare the temporal relationship between AMSR-E observations and CLM/NOAH simulations for the entire MDB, the correlation coefficient (R) and RMSE were calculated for monthly soil moisture (Figure 5). The higher the correlation coefficient and the lower the RMSE, the better agreement between two soil moisture data sets. Accordingly, over most parts of MDB, AMSR-E observations and CLM/NOAH simulations agree very well temporally. High RMSE is identified over the south-eastern parts, which is most likely because the AMSR-E observations are systematically higher than CLM/NOAH simulations during wet winter and spring (as shown in Figure 4b).

Relatively low R is observed over northern MDB, particularly across the border between QLD and NSW (region 1) and the most northern MDB (region 2). This might be related to the issue that a relatively small amount of standing water can lead to overestimated soil moisture retrievals (Walker et al., 2006), which will be discussed further in the following section.

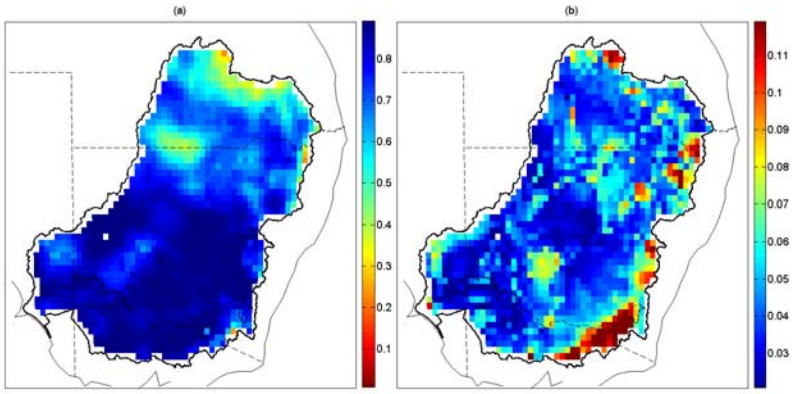

Figure 5. (a) Correlation coefficient (R) between monthly average AMSR-E soil moisture and modelling simulated soil moisture (The average of soil moisture from 2, 5, and 10-cm in CLM and 10-cm in NOAH is taken before calculating correlation coefficient) for the study period (December 2003 through November 2005) and; (b) the same as (a), but for RMSE in the unit of m^3/m^3.

The R and RMSE between point observation based precipitation and GDAS reanalysis precipitation are shown in Figure 6. In general, high correlation coefficients are observed across the entire MDB, which means that the fluctuations of rainfall between these two precipitation data sets match very well – although absolute values of precipitation might vary considerably. High RMSE is observed over the east MDB, particularly the north-eastern part. These regions have high annual precipitation, which tends to have higher discrepancies between different precipitation data sets. The differences in rainfall might explain the positive biases between CLM/NOAH simulations and AMSR-E observations over the north-east MDB (as observed in Figure 3).

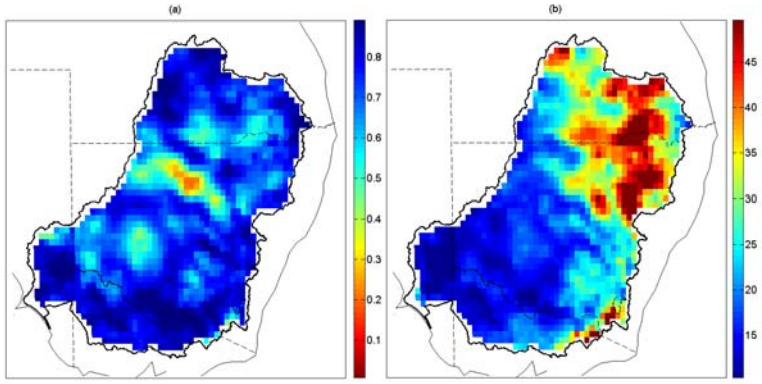

Figure 6. (a) Correlation coefficient (R) between monthly gridded precipitation from SILO and CLM/NOAH forcing precipitation for the study period (December 2003 through November 2005) and; (b) the same as (a), except for RMSE in the unit of mm/month.

4. DISCUSSION

The upward trend in AMSR-E soil moisture (Figure 4a) during the relatively dry season (summer and autumn) may be related to the seasonal variations in surface temperature and evaporation. From summer through autumn, the surface temperature decreases, as does the evaporation. Thus, the near-surface soil

moisture is expected to increase if given constant precipitation. Constant precipitation did not occur in our analysis. Most likely, this unexpected upward trend is related to the parameterization in the Land Parameter Retrieval Model, which requires further investigation.

Over the north-eastern MDB, where most precipitation events occur in summer and autumn, the AMSR-E soil moisture and model simulations agree with each other quite well (Figure 4c), but over the south-eastern MDB with high winter and spring rainfall, the AMSR-E soil moisture is systematically higher than model simulations (Figure 4b). Given the similar amount of precipitation, soil moisture during cool months is expected to be higher than that during warm months, as the surface temperature and evaporation are lower during cool months. Accordingly, soil moisture in winter in Figure 4b is expected to be higher than that in summer in Figure 4c, which can clearly be observed in the AMSR-E soil moisture retrievals, but not in model simulations. A relatively small amount of standing water can lead to overestimated soil moisture retrievals (Walker et al., 2006), through saturation of the microwave brightness temperature signal. High intensity rainfall (as can be seen in Figure 4b) is more likely to leave standing water on the surface and would greatly increase the soil moisture estimates from AMSR-E despite only a small fraction of a pixel actually being affected. This might also be due to the limit on the maximum soil moisture defined in CLM and NOAH schemes.

The low correlation coefficients in region 1 and 2 (shown in Figure 5a) may also be related to the standing water issue. The existence of large wetlands result in negative anomalies in soil moisture during summer and positive anomalies during winter, and further lead to low correlation coefficient between AMSR-E observations and CLM/NOAH simulations. It seems that the anomalies in the pixels of wetlands affect the pixels in the vicinity, which results in the low correlation coefficients to a larger scale.

This study compares near-surface soil moisture from AMSR-E observations and CLM and NOAH land surface schemes simulations from spatial and temporal aspects. Both soil moisture data sets show similar seasonal variations over the entire MDB, even though the precipitation forcing in model simulations are slightly higher than gridded rainfall products interpolated from point observations. From the temporal aspect, the best match between AMSR-E soil moisture and model simulations is found over the regions with strong precipitation in warm months, e.g. northern MDB. Over the regions with high precipitation during cool months, AMSR-E soil moisture is systematically higher than model simulations. For the regions with extremely low annual rainfall, the peak values in soil moisture between AMSR-E and model simulations match very well, but not the low values.

Both satellite observations and modelling simulations can represent the ‘true’ soil moisture to some extent. The spatial and temporal agreements between them vary under different wetting and drying conditions, and both of them have their own advantages and uncertainties. Therefore, how to blend soil moisture products from satellite observations and modelling simulations, in addition to data assimilation, will be an ongoing research task.

ACKNOWLEDGMENTS

This work was funded by the University International Postgraduate Award (UIPA) from University of New South Wales and a top-up scholarship from CSIRO Water for a Healthy Country Flagship program.

REFERENCES

Cashion, J., V. Lakshmi, D. Bosch and Jackson T. J. (2005), Microwave remote sensing of soil moisture: evaluation of the TRMM microwave imager (TMI) satellite for the Little River Watershed Tifton, Georgia. *Journal of Hydrology*, 307, 242-253.

Draper, C.S., Walker, J. P., Steinle, P.J., de Jeu, R.A.M. and Holmes, T.R.H. (2009), An evaluation of AMSR-E derived soil moisture over Australia. *Remote Sensing of Environment*, 113, 703-710.

Owe, M.., De Jeu, R., and Holmes, T. (2008), Multisensor historical climatology of satellite-derived global land surface moisture. *Journal of Geophysical Research-Earth*, 113, F01002, doi:10.1029/2007JF000769.

Rodell, M., Houser, P. R., Jambor, U., Gottschalck, J., Mitchell, K., Meng, C.-J., Arsenault, K., Cosgrove, B., Radakovich, J., Bosilovich, M., Entin, J. K., Walker, J. P., Lohmann D. and Toll, D. (2004), The Global Land Data Assimilation System. *Bulletin of the American Meteorological Society*, 85(3):381-394.

Walker, J.P., Merlin, O., Panciera, R. and Kalma, J.D. (2006), National Airborne Field Experiments for soil moisture remote sensing, *Proceedings 30th Hydrology and Water Resources Symposium*, Launceston, Tasmania, Australia.